Crystal structures of the body-centered tetragonal tectosilicates: $K_{1.14}Mg_{0.57}Si_{1.43}O_4$, $K_{1.10}Zn_{0.55}Si_{1.45}O_4$, and $K_{1.11}Fe^3_{1.11}Si_{0.89}O_4$

W. A. Dollase

Department of Earth and Space Sciences, University of California, Los Angeles, California 90024, U.S.A.
and Bayerisches Geoinstitut, Universität Bayreuth, W-8580 Bayreuth, Germany

C. R. Ross II

Bayerisches Geoinstitut, Universität Bayreuth, W-8580 Bayreuth, Germany

Abstract

The title compounds are isostructural stable phases that occur on binary joins of mineralogic interest: SiO_2-K_2MgO_2, SiO_2-K_2ZnO_2, SiO_2-$KFeO_2$; a corresponding phase occurs on the SiO_2-$KAlO_2$ join. The structure has $I4mm$ symmetry, with cell dimensions $a =$ 8.957 Å, $c = 5.281$ Å (Mg phase). The eight Si plus Mg (or Zn, Fe) atoms per cell are disordered over a single set of equivalent tetrahedrally coordinated sites. The tetrahedra form four-membered rings further interconnected into six- and eight-membered rings with two types of intervening large cavity sites: K2 sites between facing four-membered rings are full, but K1 sites in large, square channels show a smeared out partial occupancy probably caused by K-K repulsion.

The body-centered tetragonal tectosilicate (BCTT) structure is structurally related to other major tectosilicates, though no natural occurrences are yet known.

Introduction

Binary joins from SiO_2 to K_2MO_2 (M = Mg, Zn, etc.) and from SiO_2 to KRO_2 (R = Al, Fe^{3+}, etc.) contain the major structure types summarized in Table 1. These are all tectosilicates, with tetrahedrally coordinated divalent or trivalent atoms incorporated in the 3-D framework. Fundamentally they differ in the ratios of alkali cavities to tetrahedra (from 1:1 down to 0.25:1). Knowledge of individual structures and their polymorphism varies from detailed to vague.

For the structure type reported here, no crystal structure analysis has been published in the literature, though as described in the next section, some previous crystallographic data exist. Lacking a mineral name, this phase is here termed BCTT for body-centered tetragonal tectosilicate. The composition of BCTT phases is conveniently expressed as the K content per 4-O formula unit ($K_xM_{x/2}Si_{2-x/2}O_4$ or $K_xR_xSi_{2-x}O_4$). The known examples of BCTT structures have K = ca. 1.1–1.2.

Previous study

In a study of the $KAlSiO_4$-$KAlO_2$ join, Cook et al. (1977) reported unit-cell dimensions and the X-ray powder diffraction pattern (JCPDS 32-732) of a body-centered tetragonal compound of estimated composition $K_{1.1}Al_{1.1}$-$Si_{0.9}O_4$. The 1-atm phase relations along selected joins in the system K-Mg-Fe^{3+}-Al-Si-O were reported by Roth (1980a, 1980b). They found analogous tetragonal phases on the binary joins K_2MgO_2-SiO_2 and $KFeO_2$-SiO_2 and on ternary sections between these joins. They estimated phase compositions as K = $^8/_7$ in the K-Fe-Si-O system and K = $^4/_3$ in the K-Mg-Si-O system. In addition to these examples, we report here a BCTT phase at K = 1.1 on the K_2ZnO_2-SiO_2 join.

Here we report the crystal structure of this BCTT phase for the three title compositions. The tectosilicate structure that these compounds adopt has not been previously reported, although its tetrahedral connectivity has been inferred (Smith, reported in Roth, 1980b) to be of a type earlier enumerated by Wells (1954) and Smith (1977). Initial results of this study were reported in an abstract (Ross and Dollase, 1991).

Sample preparation and characterization

Synthesis experiments on the Mg- and Zn-bearing joins were carried out over the interval K = 2 to K = 1. To study the effect of substitution of trivalent atoms, a few selected compositions on the analogous Fe^{3+}-bearing join were also synthesized. Compounds were synthesized from oxide mixtures pressed into pellets and heated in covered platinumware in air to temperatures between 800 and 1200 °C for a few hours to a few days. At the highest temperatures, melts were produced and crystals or—in the Zn-bearing system—crystals and glass were recovered.

The BCTT phase was produced along with other phases in all 12 Mg-join experiments and all four Zn-join experiments between K = 1.5 and K = 1.0. On the basis of phase proportions and their changes with time and temperature, it is estimated that the Mg-BCTT phase is the single stable phase at about 1000 °C from about K = 1.17 to K = 1.10. Small consistent cell-dimension variations

TABLE 1. Structure types on the joins SiO_2-K_2MO_2 and SiO_2-KRO_2

Structure	M^{2+} composition	R^{3+} composition
Stuffed cristobalite	K_2MgSiO_4-$K_{1.5}Mg_{0.75}Si_{1.25}O_4$	$KAlO_2$-$K_{1.5}Al_{1.5}Si_{0.5}O_4$
BCTT (this study)	$K_{1.14}Mg_{0.57}Si_{1.43}O_4$	$K_{1.11}Fe_{1.11}Si_{0.89}O_4$
Kalsilite family (stuffed tridymite)	$K_2ZnSi_3O_8^*$	$KAlSiO_4$
(Unnamed)	$K_2ZnSi_4O_{10}^{**}$	?
Leucite	$K_2MgSi_5O_{12}$†	$KAlSi_2O_6$
Feldspar	?	$KFeSi_3O_8$
Silica polymorphs	SiO_2	SiO_2

Note: M = Mg, Zn, etc; R = Al, Fe^{3+}, etc.
 * Dollase and Ross (1993).
 ** Kohara and Kawahara (1990).
 † Kohn et al. (1991).

demonstrate that the BCTT phase is a solid solution. Syntheses on the Zn and Fe joins, though not performed at such close intervals, are consistent with this estimated solid-solution range. This composition range has a lower K content than that suggested by Roth for the Mg join, but it is in good agreement with previous values suggested for the Al and Fe joins (Roth, 1980a, 1980b).

Electron microprobe analyses were made on several samples cooled from melts at 1200 °C. The mean of nine analyses of a Mg sample of bulk composition K = 1.15 is $K_{1.147(8)}Mg_{0.560(6)}Si_{1.433(3)}O_4$, and the mean of six analyses of a second Mg sample of bulk composition K = 1.14 is $K_{1.151(10)}Mg_{0.561(3)}Si_{1.431(3)}O_4$. From these analyses the most probable composition (Dollase and Newman, 1984) on the SiO_2-K_2MgO_2 binary join is $K_{1.14}Mg_{0.57}Si_{1.43}O_4$, within the analytical error of both samples. The mean of three analyses of a Zn sample of bulk composition K = 1.12 is $K_{1.110(8)}Zn_{0.552(6)}Si_{1.447(4)}O_4$, which does not significantly deviate from the nearest binary join composition, $K_{1.10}Zn_{0.55}Si_{1.45}O_4$. The mean of four analyses of an Fe sample of bulk composition K = 1.14 is $K_{1.10(2)}$-$Fe_{1.12(1)}Si_{0.89(1)}O_4$, yielding a closest binary join composition of $K_{1.11}Fe_{1.11}Si_{0.89}O_4$. A Mössbauer analysis of this sample (Ross and McCammon, unpublished data) showed that all Fe is Fe^{3+}.

Mg-BCTT CRYSTAL STRUCTURE ANALYSIS

Single crystals were selected from crushed fragments of the first of the two microprobe Mg samples and tested for mosaic spread and absence of subsidiary reflections. The best of about a dozen grains was selected for further study. A set of 3646 reflections (one hemisphere, $h \geq 0$) was measured at room temperature in $\omega - 2\Theta$ mode to $(\sin \Theta)/\lambda \approx 1.0$ using graphite-monochromated Mo$K\alpha$ radiation (λ = 0.71969 Å) on an Enraf-Nonius CAD4

diffractometer. The orientation of the crystal was checked after every 300 measured reflections, and the intensities of representative reflections checked every 2 h of exposure.

Averaging of intensities in Laue class $4/mmm$ resulted in 539 unique reflections with R_{merge} = 1.9%. There is no indication of significant intensity differences between hkl and khl reflections and no significant improvement in the value of R_{merge} using Laue class $4/m$. The set of reflections indicates a body-centered lattice with no other systematic absences. Cell dimensions (Table 2) were refined from setting angles of 24 reflections, with 2Θ between 20 and 26°. The cell volume and microprobe analysis yield a calculated density of 2.54 g/cm³, Z = 4, with unit-cell content of $K_{4.56}Mg_{2.28}Si_{5.72}O_{16}$.

A starting structure was inferred from crystal chemical reasoning as follows: the short c-axis repeat of 5.3 Å, being just twice the length of a (Si,Mg)O_4 tetrahedron edge, suggests tetrahedra oriented with one edge nearly parallel to c. The fourfold axis reproduces this tetrahedron into four-membered rings, and the body centering fixes the connectivity of the rings. The alkali atoms are located in intervening large cavities.

The maximum symmetry of such an atomic array is $I4/mmm$. The diffraction symbol, however, allows five different space groups, and all were explored. Of these, only the structure in $I4mm$ could be refined to a satisfactory R factor (R = 4.2%). This particular space group selection is further supported below. The refined $I4mm$ structure is reported in Table 3.

Zn AND Fe³⁺ BCTT CRYSTAL STRUCTURE ANALYSES

The grains from the Zn- and Fe-bearing syntheses were too small and intergrown for single-crystal structure analysis. Consequently, the structures of Zn and Fe^{3+} BCTT were determined from X-ray powder data using the Rietveld method. The structure analyses took into account the small amounts of contaminant phases whose structures had been previously determined from single-phase X-ray data (Dollase and Ross, 1993; Dollase and Ross, in preparation).

X-ray powder data were obtained using a STOE diffractometer operating in transmission mode; details of diffraction hardware and data collection procedures are described in Ross et al. (1990). For the Zn sample, data

TABLE 2. Crystal data for the BCTT phases

Composition	Space group	a (Å)	c (Å)	R (%)
$K_{1.14}Mg_{0.57}Si_{1.43}O_4$	$I4mm$	8.957(1)	5.281(1)	4.2
$K_{1.10}Zn_{0.55}Si_{1.45}O_4$	$I4mm$	8.939(1)	5.246(1)	4.7
$K_{1.11}Fe_{1.11}Si_{0.89}O_4$	$I4mm$	9.102(1)	5.341(1)	5.9
$K_{1.1}Al_{1.1}Si_{0.9}O_4^*$	?	8.943(1)	5.221(1)	—

 * Cook et al. (1977).

TABLE 3. Mg, Zn, Fe BCTT crystal-structure parameters

Atoms	Site	x	y	z	β_{11}	β_{22}	β_{33}	β_{12}	β_{13}	β_{23}
2.56		0	0.5	0.296(3)	0.006(0)	0.017(2)	0.33(1)	0	0	0
2.40 K1	4b	0	0.5	0.324(38)	−0.005(3)	0.018(5)	0.57(13)	0	0	0
2.44		0	0.5	0.316(24)	0.004(3)	0.001(2)	0.48(5)	0	0	0
2		0	0	0.4979(7)	0.011(0)	β_{11}	0.023(0)	0	0	0
2 K2	2a	0	0	0.497(11)	0.014(1)	β_{11}	0.027(6)	0	0	0
2		0	0	0.496(3)	0.004(1)	β_{11}	0.014(3)	0	0	0
8 T^*		0.1805(1)	x	0	0.008(0)	β_{11}	0.021(0)	−0.001(0)	0.002(1)	β_{13}
8 T^{**}	8c	0.1818(4)	x	0	0.008(1)	β_{11}	0.022(3)	−0.001(1)	0.007(5)	β_{13}
8 $T\dagger$		0.1818(2)	x	0	0.006(1)	β_{11}	0.021(2)	−0.001(1)	−0.005(3)	β_{13}
8		0.2144(8)	0	0.0695(11)	0.027(1)	0.011(1)	0.052(2)	0	0.009(3)	0
8 O1	8d	0.2182(16)	0	0.054(13)	0.014(4)	0.013(3)	0.178(39)	0	0.015(11)	0
8		0.2212(14)	0	0.079(3)	0.019(3)	0.005(2)	0.058(12)	0	0.005(4)	0
8		0.2889(5)	x	0.1914(14)	0.025(1)	β_{11}	0.039(2)	−0.015(2)	0.009(1)	β_{13}
8 O2	8c	0.2872(17)	x	0.200(5)	0.019(4)	β_{11}	0.059(18)	−0.005(5)	−0.009(10)	β_{13}
8		0.2938(8)	x	0.180(2)	0.007(1)	β_{11}	0.028(6)	−0.001(2)	−0.006(4)	β_{13}

Note: Parameters for each atom listed in order: Mg BCTT, Zn BCTT, Fe BCTT. Anisotropic displacement form: $\exp[-(\beta_{11} \cdot h^2 + \beta_{22} \cdot k^2 + \beta_{33} \cdot l^2 + \beta_{12} \cdot hk + \beta_{13} \cdot hl + \beta_{23} \cdot kl)]$.
* $T = 2.28\text{Mg} + 5.72\text{Si}$.
** $T = 2.20\text{Zn} + 5.80\text{Si}$.
† $T = 4.44\text{Fe} + 3.56\text{Si}$.

were obtained to 140° 2Θ with a data interval of 0.02° 2Θ using $CuK\alpha$ radiation. A measured absorption coefficient, $\mu t = 0.82$, was applied during refinement. Calculated density for Zn BCTT is 2.91 g/cm³, with unit-cell contents of $K_{4.4}Zn_{2.2}Si_{5.8}O_{16}$. Because of fluorescence, the diffraction pattern of the Fe sample was measured to the same limit and data interval, using $CoK\alpha$ radiation. The measured absorption coefficient was 0.91. Calculated density for Fe^{3+} BCTT is 2.92 g/cm³, with a unit-cell content of $K_{4.44}Fe_{4.44}Si_{3.56}O_{16}$.

Rietveld refinement was performed using a slightly modified version of the program DBW (Wiles and Young, 1981). The Zn sample refinement included 19 pattern parameters: (2Θ-zero point, six background coefficients, three peak-width coefficients, pseudo-Voigt mixing term, peak asymmetry term, two tetragonal and three orthorhombic unit-cell parameters, and two scale factors), 24 structural parameters for the BCTT phase, and an overall thermal factor for the contaminant orthorhombic phase. Identical peak width and shape parameters were assumed for both phases. Initial structural parameters were taken from the Mg BCTT refinement. Refined structure parameters for Zn BCTT are included in Tables 2 and 3. The estimated standard deviations include the effect of serial correlation (Berar and Lelann, 1991). Final refinement indices are $R_p = 4.7\%$ and $R_{Bragg} = 7.9\%$. Refinement of the Fe sample involved essentially the same variables, except that two minor phases were present. Final refined structure parameters are included in Tables 2 and 3, again including the effect of serial correlation. Final refinement indices are $R_p = 5.9\%$ and $R_{Bragg} = 7.3\%$.

DESCRIPTION OF THE STRUCTURE

In the BCTT structure the eight Si plus Mg (or Zn,Fe) atoms per cell are disorderd over a single set of equivalent, tetrahedrally coordinated sites. The SiO₄ and MgO₄ (or ZnO₄,FeO₄) tetrahedra are connected by sharing all four O corners with other such tetrahedra to form a tectosilicate framework. The smallest circuit of connected tetrahedra is a four-membered ring, whose plane of T (tetrahedrally coordinated) atoms parallels (001). Tetrahedra within the ring are connected by O1 atoms and have an outer edge of O2 atoms oriented roughly parallel to the c axis. Each apex of this edge is connected to an equivalent four-membered ring related to the first one by the body-centering operation. Each four-membered ring is thus surrounded by eight other four-membered rings, as shown in Figure 1.

There are large interframework cavities of two distinct types. The two K2 sites per cell lie between parallel four-membered rings and are fully occupied. The K atoms on these sites are coordinated by eight O atoms, which form an approximate Archimedian antiprism. A second type of K site, K1, is in the large, nearly square channels that run continuously along the c axis with little change in diameter (Fig. 1a). Figure 2 shows the distance to closest O atoms for a channel-center atom located at various fractional positions, z_{K1}, along the c axis. There is a range of channel locations having the same number of similar length bonds, which yield an approximately constant bond-strength sum (Brown and Altermatt, 1985). The K1 atoms are found in the square channels along this region of near-constant coordination. In the structure refinements, the alkali distribution has been approximated by a single atom located near the center of this region, with an extremely anisotropic displacement ellipsoid. Along the [001] channel direction, K1 displacement is about four times its displacement across the channel.

The four K1 sites per cell are not fully occupied. On the basis of electron microprobe analyses, they are assigned as 2.56 K atoms in Mg BCTT, 2.40 K atoms in Zn BCTT, and 2.44 K atoms in Fe BCTT. Trial site-occupancy refinements yield similar values without significant improvement of the R factors.

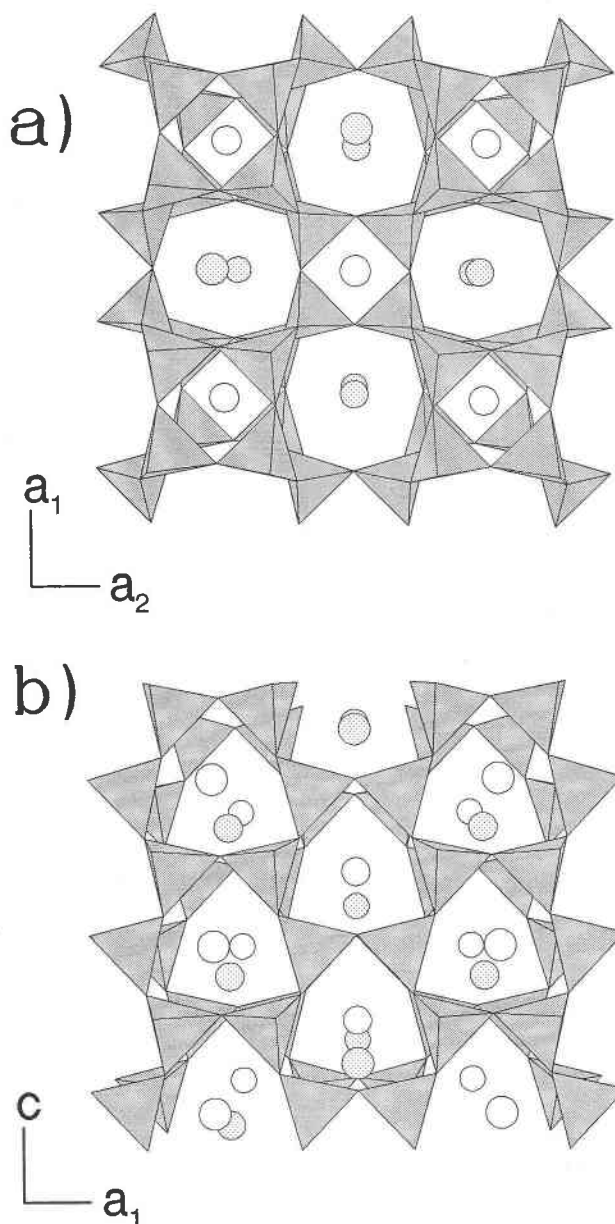Positional disorder of the K1 atoms probably helps es-

Fig. 1. Polyhedral drawing of BCTT crystal structure using Atoms (Dowty, 1989); K1 atoms are shown stippled, K2 as open circles. (a) View nearly along the c axis; (b) view nearly along the a axis.
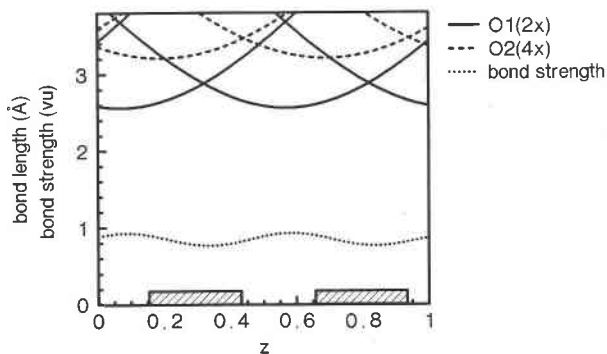

Fig. 2. Distance, number of bonds, and sum of bond strengths from O atoms to K1 atom for various channel locations, z_{K1}, in Mg BCTT. The hachured areas represent the observed K1 distribution.

tablish local charge balance disrupted by the disordered Mg(Zn,Fe)-Si distribution. The positioning of the K1 atoms along the square channels is facilitated by there being a region with relatively small differences in channel diameter, but it is also related to the total number of alkali atoms that these channels must accommodate. If the K1 sites were completely filled (requiring a different Mg/Si ratio), the composition would be K = 1.50. However, the K1 atoms would then be packed in the channels with a separation of only $c/2$ (2.6–2.7 Å) from each other, which

is too short for K atoms; partial occupancy of the channel sites relieves that difficulty.

The highly elliptical K1 distribution is repeated by symmetry every $c/2$ along the channel. Although the distance between centers of consecutive distribution ellipsoids is too short to be an acceptable K-K separation, the distance from the end of one ellipsoid to the far end of the next ellipsoid is probably acceptable (3.25 Å). If the ends of the two ellipsoidal distributions along the channel in each unit cell are serially labeled as ab cd, then the closest acceptable packing of K atoms would be Ab cD ab Cd aB cd ..., (upper case indicates occupied sites). This simple model predicts a maximum of four K atoms per three unit-cell lengths of channel and a composition of K = 1.167, which is (perhaps fortuitously) close to the observed K-rich limit.

The minimum K content of BCTT solid solution would not seem to be structurally limited. A 50% filling of the channel sites—for which close contacts could be avoided by alternate sites being empty—corresponds to K = 1.00. However, at this composition, in all the systems studied the BCTT phase is replaced by a hexagonal (or pseudohexagonal) kalsilite-related phase. The observed BCTT composition range then corresponds to the relatively small range of square-channel filling of about 60–67%.

In I4mm, as well as the other space groups allowed by the diffraction symmetry, the tetrahedral-site atoms are disordered. Lack of long-range tetrahedral ordering is consistent with the complex disparate compositional ratios (Mg/Si = 2.3/5.7, Fe/Si = 4.4/3.6) of the various BCTT compounds. Strong short-range ordering is, however, revealed by ^{29}Si MAS NMR spectra of these compounds, which will be reported in detail elsewhere (Dollase et al., in preparation).

The I4mm-averaged tetrahedral site is quite regular, as shown by the interatomic distances and angles given in Table 4. Mean T-O distances may be compared with values taken from the Inorganic Crystal Structure Database (Bergerhoff et al., 1983): Mg-O = 1.96, Zn-O = 1.95 Å. A [4]Fe^{3+}-O distance of 1.87 Å was taken from Brown

TABLE 4. Selected interatomic distances (Å) and angles (°)

	Mg BCTT	Zn BCTT	Fe BCTT
T-O1 1.688(2) 2×		1.681(12)	1.745(5)
-O2 1.707(6)		1.697(20)	1.734(8)
-O2 1.677(7)		1.619(26)	1.736(9)
Mean = 1.670			1.740
O1-T-O1 107.4(4)		110.2(18)	109.4(6)
O1-T-O2 108.3(4) 2×		109.0(20)	107.7(6)
O1-T-O2 109.8(3) 2×		107.1(23)	109.4(5)
O2-T-O2 113.0(3)		114.3(11)	113.4(4)
T-O1-T 147.2(4)		150.4(29)	143.1(8)
T-O2-T 139.7(4)		142.3(12)	134.2(5)
K1-O1 2.827(10) 2×		2.79(9)	2.90(6)
-O1 2.941(10) 2×		2.89(10)	2.84(5)
-O2 3.256(5) 4×		3.26(4)	3.35(2)
K2-O1 2.971(7) 4×		3.03(7)	3.00(2)
-O2 2.866(5) 4×		2.90(3)	2.83(1)

and Altermatt (1985). Combining these values with a distance of 1.61 Å for Si-O yields expected mean T-O bond lengths of 1.71, 1.70, and 1.75 Å for the Mg, Zn and Fe^{3+} BCTT phase, respectively. The observed mean values (Table 4) are close to, but uniformly slightly shorter than, those expected. Correction of the BCTT observed distances for correlated thermal (and positional disorder) displacement would slightly increase the instantaneous T-O values, further improving the agreement.

Displacement ellipsoid axial lengths, orientations, and equivalent isotropic temperature factors may be calculated from the anisotropic displacement coefficients included in Table 3. Values derived from powder data are similar to the Mg-BCTT values discussed below but are much less precise. Displacement amplitudes are large because of the disorder. Because Mg-O bond lengths differ from Si-O bond lengths by about 0.33 Å, there must be disorder displacement of individual T and O atoms of at least half this difference.

Cations show relatively isotropic displacement amplitudes (with the exception of the K1 distribution discussed above). O atoms, on the other hand, show the expected anisotropy resulting from the framework connectivity in which the shortest displacement axis tends to parallel the T-T vector, the intermediate axis tends to lie in the T-O-T plane normal to T-T, and the longest axis tends to be normal to the T-O-T plane. This model is followed approximately in the BCTT structure; for the Mg compound, the shortest O1 displacement axis is along the T-T vector, the longest axis is normal to the T-T vector, and similarly, the longest displacement axis of O2 is normal to the (110) plane, which contains the T-O2-T linkage.

STRUCTURE COMPARISON AND SYMMETRY

The structural changes with composition are related to the distortion of the real structure from the aristotype. The reduction from the highest possible symmetry of this framework ($I4/mmm$) to that observed ($I4mm$) results from the rotation of the tetrahedra in (110) about the T atoms. Figure 3a shows a section through the ideal $I4/mmm$ structure along (110). Shaded tetrahedra are those
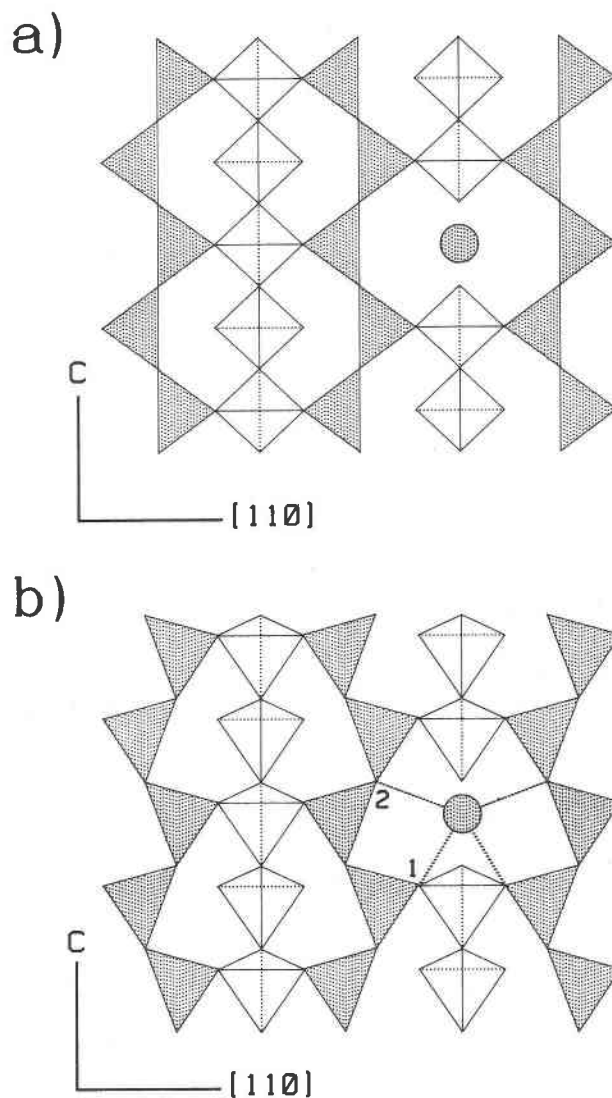
Fig. 3. Projections on (110) of (a) the aristotype, and (b) the actual BCTT structure. Dashed lines indicate bonds to a K2 atom (stippled circle) from O1 and O2.

lying directly on the (110) mirror plane, whereas the unshaded tetrahedra lie just above or below this mirror. In this configuration, a K1 atom (as shown) would be 16-fold-coordinated with K-O bond lengths of 3.3 and 3.4 Å. Both the coordination number and distances are substantially larger than typical K environments (see, e.g., Smyth and Bish, 1988).

In the real structure (Fig. 3b), the TO4 groups rotate in (110) by about 20° from their fully extended $I4/mmm$ configuration. Through corner sharing, rotation of one tetrahedron in a chain causes a counter rotation of the next tetrahedron, and so on. This pattern of rotation moves half the coordinating O1 and O2 atoms toward a K2 atom and half away (toward another K2 atom in an adjoining cage). As a result, the coordination number of

K2 atoms decreases to 8, with K-O bond lengths becoming 2.9–3.0 Å. These values are typical for K in silicates (Smyth and Bish, 1988).

In addition to accommodating the K2 bonding requirements, this rotation also reduces the T-O2-T angle from 180 to about 140°, making it similar to the T-O1-T angle in the same structure and to T-O-T angles usually found in framework silicates. Because of the (mean) tetrahedron size differences, the amount of rotation differs for the three compounds: 19.7° for Zn BCTT, 20.5° for Mg BCTT, and 24.5° for Fe^{3+} BCTT.

Such tetrahedral rotation, satisfying the K2 bonding, is not possible in $I4/mmm$ nor in any of the tetragonal subgroups other than $I4mm$. In each of those cases, the TO_4 group is fixed by symmetry and unable to rotate, or in the case of $I\overline{4}2m$, the tetrahedron could rotate but only about the O1 atom (which is constrained to lie on a twofold axis), and such rotation would not change the K2-O1 distance.

The minor cell dimension differences and the striking similarity of the Mg BCTT powder pattern with the published powder pattern of the isoelectronic Al-bearing phase (Cook et al., 1977) suggest nearly identical crystal structures, albeit with different tetrahedral site occupancies. X-ray powder diffraction patterns of the three compounds reported here have been deposited in the JCDPS powder diffraction data file.

TETRAHEDRAL CONNECTIVITY: PREVIOUS STUDIES

Wells (1954) derived a large number of possible three-dimensional, four-connected nets, including the net with the connectivity of the BCTT phase (his Table 2, net no. 7; see also his Fig. 12). At that time there were no known structures with this tetrahedral connectivity. Smith (1977), in an enumeration of three-dimensional, four-connected nets, also listed the symmetry ($I4/mmm$) and approximate cell dimensions of a tetrahedral net of this connectivity (his net no. 3). Smith (quoted in Roth, 1980b) noted that the tetragonal phase of Cook et al. (1977) could correspond to Smith's net no. 3; this prognosis is here confirmed.

Smith (1977) noted this net type was found in monoclinic $CaAl_2Si_2O_8$ (Takéuchi et al., 1973). The Ca compound has space group $P2_1$, a proper subgroup of the space group of the ideal tetrahedral linkage. Substitution of Ca for K results in partial framework collapse around the smaller (sixfold- to sevenfold-coordinated) Ca atoms as well as major site occupancy differences. There are only about 0.48 Ca atoms per four-O formula unit compared with 1.14 K in Mg BCTT. The K2 site between two facing four-membered rings, though completely filled in the BCTT structure, is highly distorted and empty in the Ca-bearing structure. All Ca atoms are found in the [001] channels. In Mg BCTT, the (K1) channel sites are about 64% filled, whereas in the Ca compound the analogous channel sites are about 48% filled. The positions of the atoms along the channels also markedly differ in the two structures.

REFERENCES CITED

Begerhoff, G., Hundt, R., Sievers, R., and Brown, I.D. (1983) The inorganic crystal structure database. Journal of Chemical Information and Computer Sciences, 23, 66–69.

Berar, J.F., and Lelann, P. (1991) E.S.D. and estimated probable error obtained in Rietveld refinements with local correlations. Journal of Applied Crystallography, 24, 1–5.

Brown, I.D., and Altermatt, D. (1985) Bond-valence parameters obtained from a systematic analysis of the inorganic crystal structure database. Acta Crystallographica, B41, 244–247.

Cook, L.P., Roth, R.S., Parker, H.S., and Negas, T. (1977) The system $K_2O-Al_2O_3-SiO_2$. 1. Phases on the $KAlSiO_4-KAlO_2$ join. American Mineralogist, 62, 1180–1190.

Dollase, W.A., and Newman, W.I. (1984) Statistically most probable stoichiometric formulae. American Mineralogist, 69, 553–556.

Dollase, W.A., and Ross II, C.R. (1993) Crystal structure of $K_2ZnSi_3O_8$. Zeitschrift für Kristallographie, in press.

Dowty, E. (1989) ATOMS: A computer program for displaying atomic structures. Shape Software, Kingsport, Tennessee.

Kohara, S., and Kawahara, A. (1990) Structure of synthetic dipotassium zinc tetrasilicate. Acta Crystallographica, C46, 1373–1376.

Kohn, S.C., Dupree, R., Mortuza, M.G., and Henderson, C.M. (1991) An NMR study of structure and ordering in synthetic $K_2MgSi_5O_{12}$, a leucite analogue. Physics and Chemistry of Minerals, 18, 144–152.

Ross II, C.R., and Dollase, W.A. (1991) Crystal structure of $K_{1.16}Mg_{0.58}Si_{1.42}O_4$, a new tectosilicate structure type. American Geophysical Union Fall Meeting Program and Abstracts, 1991, 554.

Ross II, C.R., Rubie, D.C., and Paris, E. (1990) Rietveld refinement of the high-pressure polymorph of Mn_3O_4. American Mineralogist, 75, 1249–1252.

Roth, R.S. (1980a) Phase equilibria research in portions of the system $K_2O-MgO-Fe_2O_3-Al_2O_3-SiO_2$. In S.L. Holt, J.B. Milstein, and M Robbins, Eds., Solid state chemistry: A contemporary overview, p. 391–408. Advances in chemistry series 186, American Chemical Society, Washington, DC.

———(1980b) In R.S. Roth, J.R. Dennis, and H.F. McMurdie, Eds., Phase diagrams for ceramists, vol. VI, Figs. 6552, 6555, 6557. American Ceramic Society, Westerville, Ohio.

Smith, J.V. (1977) Enumeration of 4-connected 3-dimensional nets and classification of framework silicates. I. Perpendicular linkage from simple hexagonal net. American Mineralogist, 62, 703–709.

Smyth, J.R., and Bish, D.L. (1988) Crystal structures and cation sites of the rock-forming minerals, p. 319–320. Allen and Unwin, Boston.

Takéuchi, Y., Haga, N., and Ito, J. (1973) The crystal structure of monoclinic $CaAl_2Si_2O_8$: A case of monoclinic structure closely simulating orthorhombic symmetry. Zeitschrift für Kristallographie, 137, 380–398.

Wells, A.F. (1954) The geometrical basis of crystal chemistry. Part 2. Acta Crystallographica, 7, 545–554.

Wiles, D.B., and Young, R.A. (1981) A new computer program for Rietveld analysis of X-ray powder diffraction patterns. Journal of Applied Crystallography, 14, 149–151.